Nucleic Acids Research, 1995, Vol. 23, No. 3 351–356

Identification of close contacts between the σ^N (σ^{54}) protein and promoter DNA in closed promoter complexes

Wendy Cannon, Sara Austin, Madeleine Moore[1] and Martin Buck*

AFRC-IPSR Nitrogen Fixation Laboratory, University of Sussex, Falmer, Brighton BN1 9RQ, UK and [1]Department of Chemistry, York University, Hesslington, York YO1 5DD, UK

Received November 16, 1994; Revised and Accepted December 16, 1994

ABSTRACT

The complexes forming between the alternative sigma factor protein σ^N (σ^{54}), its holoenzyme and promoter DNA were analysed using the hydroxyl radical probe and by photochemical footprinting of bromouridine-substituted DNA. Close contacts between the promoter, σ^N and its holoenzyme appear to be restricted predominantly to one face of the DNA helix, extending from –31 to –5. They all appear attributable to σ^N and no extra close contacts from the core RNA polymerase subunits in the holoenzyme–promoter DNA complex were detected. We suggest that the apparent absence of close core RNA polymerase contacts in the region of the promoter DNA to be melted during open complex formation is important for maintaining the closed complex. Results of the hydroxyl radical footprinting imply that σ^N makes multiple DNA backbone contacts across and beyond the –12, –24 consensus promoter elements, and the photochemical footprints indicate that consensus thymidine residues contribute important major groove contacts to σ^N. Formation of the open complex is shown to involve a major structural transition in the DNA contacted by σ^N, establishing a direct role for σ^N in formation of the activated promoter complex.

INTRODUCTION

In prokaryotes RNA polymerase is directed towards promoter sequences by specific DNA-binding σ factor proteins (1). σ^N proteins (also called σ^{54}) are an alternative family of σ factors displaying no significant homology to the major σ family (2), of which the σ^{70} vegetative σ factor of *Escherichia coli* is a typical member (3). Although the proteins of both σ families interact with a common core RNA polymerase, the resulting holoenzymes have very distinctive properties (4). Promoter recognition elements for the σ^N–holoenzyme are located around –12 and –24 instead of the usual –10, –35 used by σ^{70}–holoenzyme and are themselves distinct sequences (see 5, and Fig. 1). Once bound to promoter DNA, the σ^N–holoenzyme complex remains as a stable closed promoter complex only isomerising to the open complex, in which the DNA around the transcription start site is locally denatured, when acted upon by an enhancer-binding activator protein (5–7). The role of the activator protein in σ^N-dependent transcription initiation suggests similarities to the eukaryotic Pol II initiation mechanism (2).

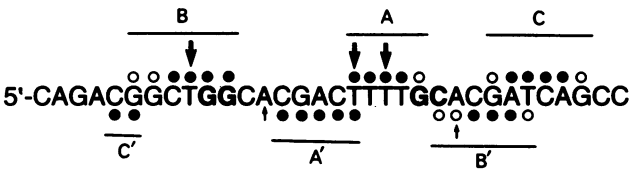

Figure 1. The *R.meliloti nifH* promoter sequence from –35 to –3 and regions protected from chemical attack by σ^N. Symbols above the sequence indicate top strand reactivities, symbols below bottom strand reactivities. Filled circles: strong hydroxyl radical protection; open circles: weaker hydroxyl radical protection. Large arrows: strong suppression of 5-bromouridine reactivities; small arrows: weaker suppression. Protected regions B, A and C and B′, A′ and C′ correspond to those shown in Figures 4 and 6. Consensus promoter elements are 5′-CTGGCAC from –28 to –22 and TTTGCA from –17 to –12, containing the GG and GC dinucleotides respectively, which characterise σ^N binding sites (5,11).

Extensive deletion and point mutagenesis analyses of σ^N from *E.coli* and *Klebsiella pneumoniae* have led to the conclusion that the DNA-binding function of σ^N resides in the C-terminus and involves a helix–turn–helix DNA-binding motif (8–10). The DNA-binding determinants of σ^N are functional in the isolated protein (11), in contrast to σ^{70}, where they appear masked until the holoenzyme forms (12). Although σ^N binds specifically to the same promoter sequences recognised by its holoenzyme form, the DNA adjacent to the –12 promoter element appears locally distorted in the holoenzyme complex (13). This DNA distortion is core-dependent and also requires the integrity of the N-terminal Region I of σ^N, a glutamine-rich region whose role in σ^N function is not that of the primary core-binding determinant (10,13–17). Rather, Region I appears to be important for activation, which

* To whom correspondence should be addressed at present address: Department of Biology, Imperial College of Science, Technology and Medicine, Prince Consort Road, London SW7 2BB, UK

may involve establishing the nucleation of DNA strand separation within the closed complex (13).

We have now probed promoter complexes with σ^N and its holoenzyme using the hydroxyl radical (18) and also 5-bromouridine-substituted DNA (19) to visualise close protein–DNA contacts. Results establish that σ^N and holoenzyme sit on one face of the DNA helix and that a number of T residues important for determining the affinity of the promoter as a binding site for σ^N (5) appear to contribute major groove contacts to σ^N and holoenzyme (see Figs 1 and 6). The apparent absence of close contacts between core RNA polymerase subunits and promoter DNA may be important for maintaining the promoter–holoenzyme complex as a closed complex. Distortion of the DNA within the closed promoter complex is likely to involve a core RNA polymerase-mediated adjustment of σ^N conformation. We also show that open complex formation involves direct contacts between σ^N and the melted DNA region.

MATERIALS AND METHODS

Proteins

These were prepared as described previously and are the *K.pneumoniae* σ^N protein and core RNA polymerase (20). σ^N was over-produced from a modified construct in which the native *rpoN* ribosome-binding site was replaced with a consensus site (plasmid pWVC93025). Briefly, the linkers 5′-AATTCAGGAGG, 3′-GTCCTCC replaced the *Eco*RI–*Hae*III fragment of the *rpoN* gene in pMM38 (20). Expression was driven by the *tac* promoter of pDK5 (21). Glycerol was removed from proteins used in hydroxyl radical footprinting by dialysis against 25 mM Tris–acetate, pH 8.0, 10 mM KCl, 0.1 mM dithiothrietol (DTT), for 6 h. For core RNA polymerase 60 mM KCl was also present.

Template DNA

The *Rhizobium meliloti nifH* promoter (Fig. 1) was used in the footprinting experiments and 5′-end labelled DNA was prepared by extending single-stranded DNA of M13mp18- or mp19-derived clones (20). Formation of 5-bromouridine-substituted DNA was achieved by polymerisation of a deoxynucleotide mixture in which 5-bromouridine 5′-triphosphate replaced the usual nucleotide (11).

Footprints

Footprints on bromouridine-substituted templates were conducted as described (22) except that the irradiation time was reduced to 10 min. After proteinase K treatment samples were phenol extracted twice, precipitated and then dissolved in loading dye for gel electrophoresis.

Hydroxyl radical footprinting was conducted in 25 mM Tris–acetate, pH 8.0, 8 mM Mg-acetate, 10 mM KCl, 1 mM DTT with 1.6 nM template (≈150 000 d.p.m. by dry Cerenkov counting), 50 µl final volume. σ^N was present at 960 nM, holoenzyme at 600 nM (prepared by combining σ^N and core RNA polymerase in a ratio of 1.5:1). After incubation at 30°C for 20 min, 5 µl of 0.5 mM $(NH_4)_2Fe(SO_4)_2.6H_2O$, 1.0 mM EDTA was added followed by 5 µl of 10 mM Na-ascorbate and 5 µl of fresh 0.3% H_2O_2 to the tube wall (18). The reagents were gently mixed in, and after 1 min, 121 µl of stop reagent (5 µl of 0.1 M thiourea, 16 µl of 0.2 M EDTA, 2.5 µg tRNA, 100 µl of 0.3 M Na acetate) was added to terminate the reaction. Samples were ethanol precipitated, washed and dissolved in 50 µl of 10 mM Tris–HCl, 0.1 mM EDTA, pH 8.0, to which 1 µl of 0.4% SDS and 0.5 µg of proteinase K were added at 37°C for 1 h. Samples were then phenol:chloroform:isoamylalcohol extracted, ethanol precipitated and finally dissolved in 8 µl 10 mM Tris–HCl, 0.1 mM

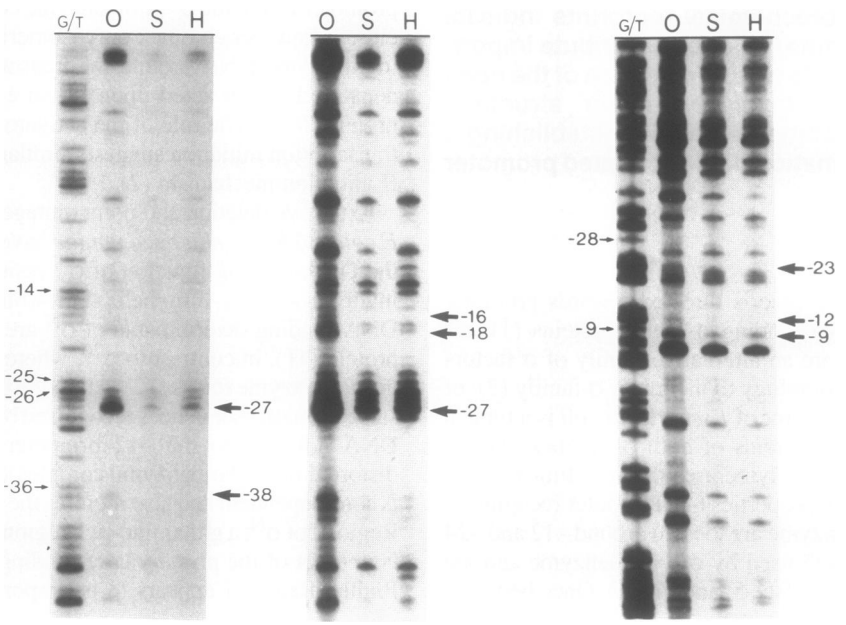

Figure 2. Suppression of the reactivity of 5-bromouridine-substituted DNA by the binding of σ^N and its holoenzyme. GT is a chemical sequencing ladder; O, no protein; S, σ^N; H, holoenzyme. Clear suppression at –16, –18 and –27 is evident on the top strand (first two panels), very weak suppression at –23, –12 and –9 on the bottom strand (third panel). Some weak suppression around –38 is also evident on the top strand. Two exposures of the top strand gel are shown to illustrate the –16, –18 and –27 suppression data.

EDTA, pH 8.0, plus 4 µl of formamide loading dye for electrophoresis.

Open complex footprints were conducted as previously described (13), but in the absence of the integration host factor (IHF) protein because we wished to examine only the polymerase footprint (see also 30). Similarly, *o*-copper phenanthroline footprints were conducted (13), except that the buffer conditions and proteins prepared for hydroxyl radical footprinting were employed.

RESULTS

Identification of contacted thymidine residues

The use of bromouridine-substituted DNA allows the probing of DNA–protein complexes at high resolution *in vitro* (19). In the absence of bound protein, irradiation of the substituted DNA results in the formation of a uridine radical at the 5 position, which abstracts a proton from the neighbouring sugar on the 5′ side and then decomposes to give 5′-dU termini, generating a DNA fragment from strand breakage. In the presence of protein, suppression of strand breakage may occur by formation of a crosslink to the reactive free radical form of uridine or by donation of a hydrogen atom to the free radical. In either case, suppression implies that that protein lies close to the 5-methyl group of thymidine. A functional role for the 5-methyl group in binding σ^N was suggested on the basis of results showing that substitution of cytidine by 5-methylcytidine increased σ^N binding, whereas substitution of deoxyuridine for thymidine decreased σ^N binding. The C and T residues were at positions in the consensus sequence most frequently occupied by T (11).

Figure 2 shows the fragment patterns resulting from the irradiation of 5-bromouridine-substituted promoter DNA in the presence or absence of σ^N and its holoenzyme. Chemical sequencing ladders employing piperidine cleavage were used to assign break positions, taking into account that the fragments resulting from light-induced chain breakage are one base shorter because the break is at the sugar 5′ to the 5-bromouridine (chemically it is the sugar attached to the 5-bromouridine). As observed in other systems (19), the reactivity of the naked DNA is not equivalent throughout, and the residue at position –18, the 5′ end of the T tract preceding the GC –12 promoter element, is significantly more reactive than those residues at –17, –16 and –15. Pyrimidine dimer formation across this promoter element also indicated that the T residues of this region were not all equivalent (22). In the presence of σ^N the reactivities at –27, –18 and –16 on the top strand were clearly suppressed. The footprint of the holoenzyme was very similar. Weak suppression in the –38 region of the promoter was also evident for both σ^N and holoenzyme. This may indicate a transient interaction of this promoter region with σ^N and holoenzyme, perhaps some wrapping of the DNA with the major groove facing the protein at this point. Reactivities of bottom strand DNA did not change as markedly as the top strand when σ^N or holoenzyme were included in the footprint assays. However some suppression at –12 and –23 was just evident. As with the top strand footprint, the holoenzyme and σ^N footprints were very similar. These data are summarised in Figures 1 and 6, together with the hydroxyl footprints. In conclusion, it appears that σ^N closely approaches the major groove of the consensus promoter elements to contact specific thymidine residues, and in the case of the TTTTGCA sequence from –18 to –12 contact at alternate T residues (–18 and –16)

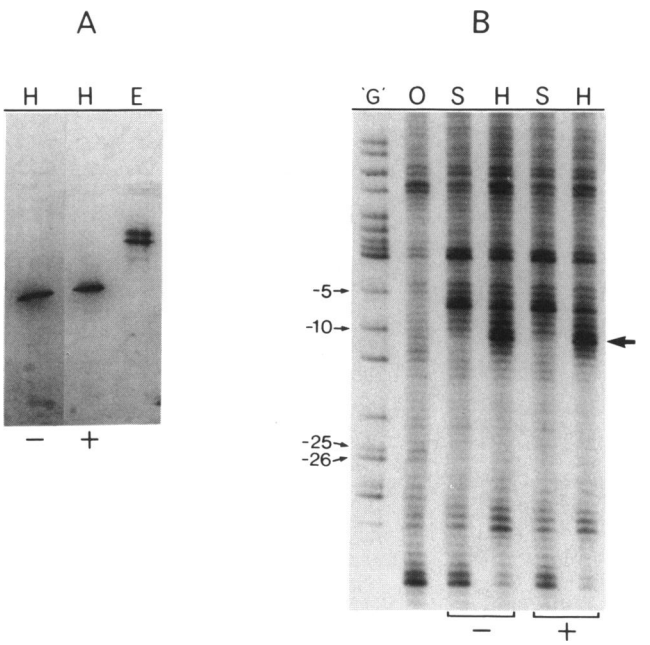

Figure 3. Formation and activity of holoenzyme under conditions used for hydroxyl radical footprinting. (**A**) native gel showing that core RNA polymerase (E) combines with σ^N to form holoenzyme (H). In this assay proteins were resolved on a 4–15% native Phastgel (Pharmacia) and Coomassie stained. (–) holoenzyme assembled from core and σ prepared for hydroxyl radical footprinting; (+) holoenzyme assembled from core (E) and σ prior to dialysis (see Materials and Methods). The dialysed core RNA polymerase had a similar mobility to that of the undialysed material (data not shown). Under our assay conditions, core RNA polymerase is resolved into two major components with several other minor components being present. Whether they represent different conformations of the same subunit composition or different associations of the subunits was not distinguished. (**B**) *o*-copper phenanthroline footprints conducted under hydroxyl radical footprinting conditions using proteins prepared without glycerol (–) or with glycerol (+). Extra cutting around –12 (arrowed) is evident in both cases and is diagnostic of holoenzyme (H) binding, but is absent from σ (S) footprints. G is a chemical sequencing ladder.

implies a structural role for the residues at –17 and –15 as suggested earlier for the TGCA sequence (13).

Protection of the DNA backbone by σ^N

Cleavage of the DNA backbone by the hydroxyl radical involves direct attack on the ribose with a reagent similar in size to a water molecule and thus is effective at detecting intimate contact between protein and DNA. Importantly, the hydroxyl radical reagent can provide information about the sidedness of the binding of protein to DNA, which is not readily obtained with DNase I footprinting. We ensured that the holoenzyme would form and bind the promoter under the assay conditions used. Firstly (see Fig. 3) the σ^N and core RNA polymerase prepared for hydroxyl radical footprinting were shown to combine and form holoenzyme by the native gel assay in which the mobility of σ^N and core RNA polymerase are distinct from holoenzyme (15). Additionally, under the conditions used for hydroxyl radical footprinting, *o*-copper phenanthroline footprints showed the expected enhanced reactivity around –12 which is diagnostic of holoenzyme binding (but not σ^N or core RNA polymerase) to the promoter (Fig. 3) (13). In conclusion, we are confident that the holoenzyme is formed and occupies the promoter under the footprinting conditions employed.

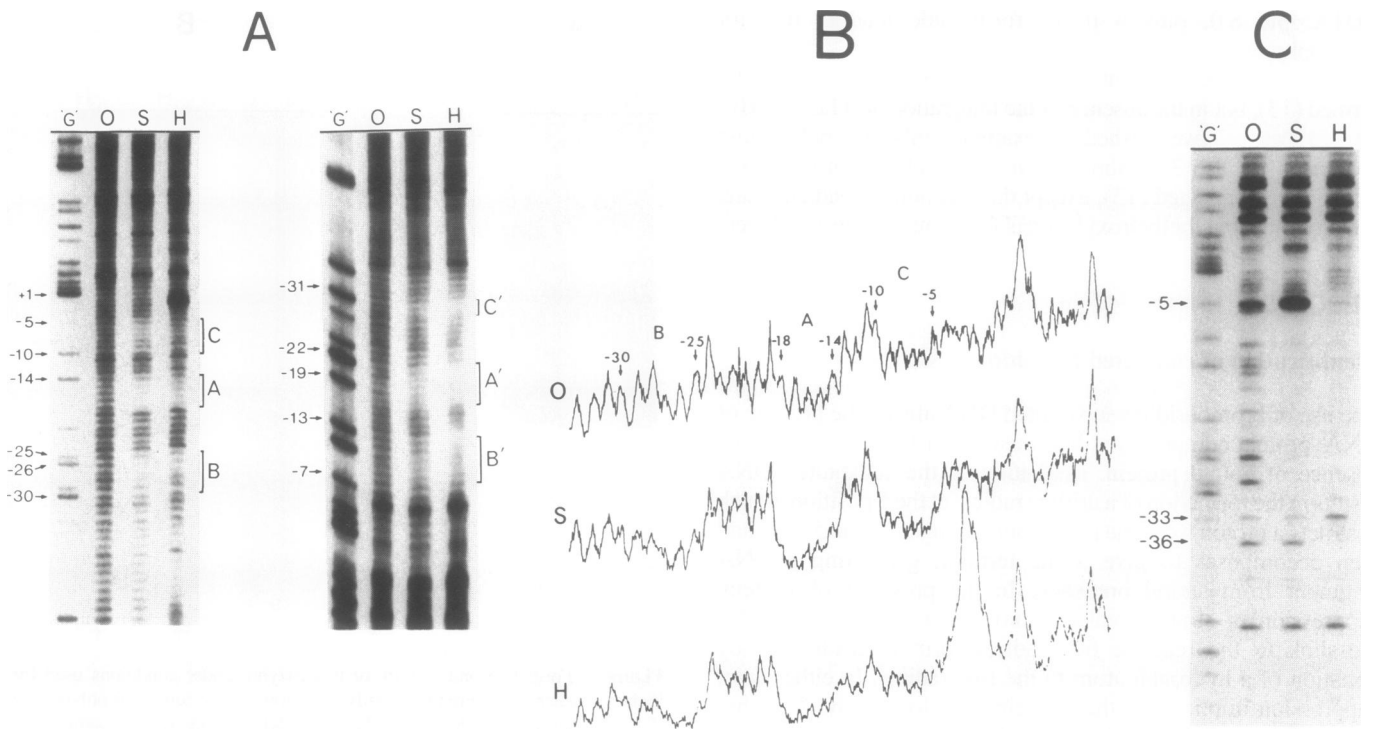

Figure 4. (**A**) Protection of promoter DNA backbone by σ^N and holoenzyme revealed by hydroxyl radical footprinting. G is a chemical sequencing ladder; O, no protein addition; S, σ^N; H, holoenzyme. Three protected regions are evident, B, A and C (top strand) and B′, A′ and C′ (bottom strand), covering the consensus promoter regions (see also Fig. 1). (**B**) Densitometer scans of the top strand footprint autoradiographs. (**C**) DNase I footprints reveal extra cutting around –33, and protection around –36 in the complex with holoenzyme (H) but not with σ^N alone (S). The extents of hydroxyl radical and DNase I footprints are very similar. G is a sequencing ladder. In other studies on holoenzymes, small differences in the upstream footprint boundary were detected with DNase I but not with the hydroxyl radical (39).

The hydroxyl cleavage products shown in Figure 4A and B were assigned directly using chemically cleaved DNA, since both chemistries yield 3′-P ends. The extent of protection afforded by σ^N and its holoenzyme is in good agreement with data from DNase I and exonuclease III footprints (11,13). Footprints revealed three regions of protection: A, B and C for the top strand and A′, B′ and C′ for the bottom strand. These are summarised in Figures 1 and 6. Comparison of σ^N and holoenzyme footprints did not show any significant reproducible differences. The extra cutting seen with holoenzyme around –2 was not consistently observed in all experiments. The protection afforded by σ^N and its holoenzyme in regions B′C and A′A may be related across the minor groove, since the cutting shows a 3′-offset of three bases (backbone positions closest to each other are 3 bp apart in sequence). This is clearly not so for the upstream protections around region C′B, which is extremely strand asymmetric. Thus although σ^N probably crosses the minor groove of the downstream promoter region, it does not appear to at the upstream promoter region. The hydroxyl radical footprints show that σ^N binds to one face of the DNA helix (Fig. 6), and although DNase I footprints do not reveal this, the extra DNase I cutting evident at –33 does indicate that at the upstream promoter region the minor groove is facing away from σ^N in the holoenzyme (Fig. 4C). The extent of contact detected by the hydroxyl radical footprinting is consistent with a B DNA-binding cleft or surface around 75 Å long. The size of the σ^N–DNA crosslinked product (17) indicates that σ^N contacts DNA as a monomer.

A σ^N-contacted region is melted in the activated complex

The σ^N–holoenzyme bound at the *R.meliloti nifH* promoter was activated by the addition of the positive control protein NifA and the hydrolysable nucleoside triphosphate dideoxyATP (which would not allow initiation of the activated complex). By using $KMnO_4$ as the probe for melted DNA (23) the T residue at –8 became highly reactive in the activated complex (Fig. 5) and adjacent C-7 also increased in reactivity. This result establishes that a σ^N-contacted region of the promoter undergoes a major structural transition under the conditions required for formation of the open promoter complex. Previous work had suggested that σ^N would interact with the promoter region downstream of –12 (13) and that this interaction would be influenced by the activator protein (24).

DISCUSSION

The binding of σ^N to its target promoter sequences in the absence of core RNA polymerase allows identification of specific σ^N–DNA contacts. Additionally, the influence of core RNA polymerase upon the σ^N–DNA interaction can be evaluated. The composite map of DNA contacts shown in Figure 6 summarises the major groove and backbone protection data for the *R.meliloti nifH* promoter. To date no clear evidence implicates σ^N contact to base functional groups accessible in the minor groove (24), although it should be noted that the minor groove-specific reagent *o*-copper phenanthroline appears excluded from promoter DNA

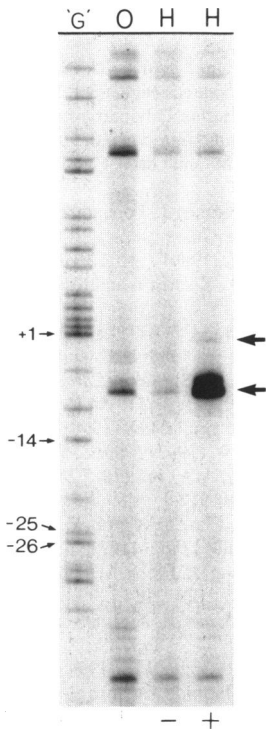

Figure 5. DNA melting in the σ^N-protected downstream promoter region. Complexes were probed with $KMnO_4$ to detect distorted T residues (and C residues). G, a chemical sequencing ladder; O, no protein; H[–], closed promoter complex (holoenzyme plus DNA); H[+], activated promoter complex (by addition [+] of NifA and ddATP). Reactive T residues at –8 and –1 are shown (arrows). The C at –7 also increased in reactivity, but was not well resolved in the autoradiograph.

across the majority of sequence footprinted with DNase I or exonuclease III (13). Major groove sequence-specific contacts appear restricted to the –27 to –12 region of the promoter, in agreement with the consensus σ^N binding site (Fig. 1) comprising this region of the promoter. Since Br is a good analogue of the methyl group, having a Van der Waals radius of 1.95 Å compared to 2.0 Å, the T residues at –27, –18 and –16 probably establish Van der Waals contacts with σ^N. A higher density of major groove contacts is detected around the –24 promoter element than the –12 region. In contrast, the downstream promoter region has a higher density of backbone contacts. This implies that the appropriate backbone configuration is important for σ^N binding, and that it may be the major factor for contacts downstream of –12, where major groove contacts are not evident. This does not discount minor groove contacts, which lack the potential for strong sequence discrimination. Contact downstream of –12 is predicted to be largely sequence-independent.

The footprint made by a conventional single helix–turn–helix would predictably shadow the two DNA strands to give related backbone protections, e.g. the patches A′A or B′C, but not both (25). The proposed recognition of the downstream –13 promoter region by a helix–turn–helix structure in σ^N (8) and the observed footprints suggest that such a structure may either constitute only part of the σ^N binding cleft interacting with the downstream –13 promoter region or establish a large number of backbone contacts. Protections C′B are consistent with the simple interaction of a single helix–turn–helix structure at the –24 promoter part, but genetic evidence interpreted as indicating an interaction between the –13 promoter region and a helix–turn–helix (8) would suggest a different feature of the DNA binding cleft interacts at the –24 region.

At present it is not possible to establish whether the backbone contacts involve for example hydrogen bonding NH groups of the σ^N peptide main chain or basic amino acids interacting with the phosphates. However, for one major groove contact, at –16, methylation protection of G at this position in the *nifJ* promoter (26) and suppression of 5-bromouridine reactivity (this study) implies that the amino acid(s) contacting this residue must be able both to H-bond and to establish a Van der Waals contact. It is also likely that contact at –16 is important in establishing the DNA conformational change detected at this position when either σ^N

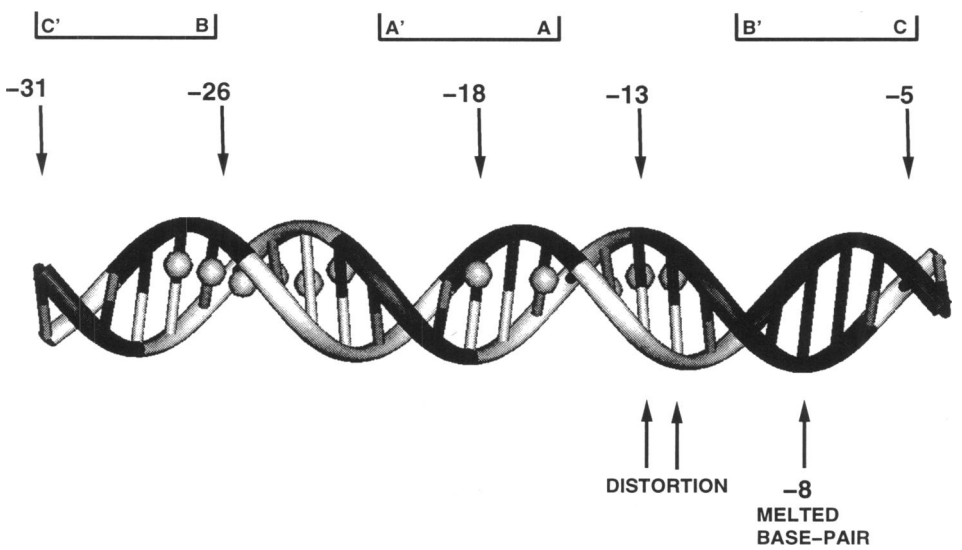

Figure 6. Summary helical map showing that the backbone protections are located on one B DNA helix face (shaded portion of figure). The –12 promoter region distorted in the closed complex lies between protections A′A and B′C, and the –8 melted region in the activated complex within protection B′C (see also Fig. 1). Major groove contacts (filled spheres) are those inferred from dimethylsulphate footprinting experiments (see 5,11,13,15; also 6) and 5-bromouridine footprints (this paper). These are bases at –27 to –22 and –18, –16, –14 to –12. Backbone contacts are both on the outer sides of and also connect to the recognition grooves defined by these base contacts. Base contact spheres at –24 and –14 are partially hidden in the figure.

or holoenzyme bind (22). In the case of the additional core-dependent conformational change in promoter DNA detected by *o*-copper phenanthroline footprinting (13, and see also Fig. 3B), which involves bases immediately downstream of the GC element, no extra core-dependent contacts were detected, implying that the transition in DNA structure is brought about by core RNA polymerase modifying the conformation of σ^N. Core RNA polymerase could organise by allostery or directly contribute to the putative DNA-binding cleft of σ^N. The distorted region around –12 appears not to be tightly contacted by σ^N; hydroxyl attack is only partly blocked and the major groove contact signal is weak, consistent with DNA contacts from σ^N either side of the deformed region being mainly responsible, in combination with core polymerase, for bringing about the change in DNA structure.

Activation of transcription at σ^N-dependent promoters is face-of-the-helix-sensitive (27,28), and the activator protein appears to contact the closed complex through DNA looping (29, see also 30,31). Since σ^N and holoenzyme occupy only one face of the DNA helix, it is formally possible that the activator approaches polymerase from the open face of the promoter and could itself be involved in a DNA transaction during catalysis of open complex formation, in addition to engaging the polymerase. The latter appears crucial in that a conformational change in the holoenzyme must accompany opening of the promoter to allow the catalytic core subunits to contact the melted region. In our assay system the distortion at –8 in the activated complex occurs in a promoter region contacted by σ^N. This clearly implies a direct role for a σ^N–DNA contact in formation of the open complex, and in all probability a change in σ^N conformation also. Thus σ^N may be one target for the activator protein. Regions of the α subunit of RNA polymerase required for activation of σ^{70} holoenzyme do not appear essential for σ^N–holoenzyme activation (32). It is notable that T7 RNA polymerase discriminates between promoters using contacts at –10, –11, –12 and –15, and like σ^N, lies over the region to be melted in models of the binary complex, implying a similar broad organisation of DNA-contacting elements in the two proteins (33–35). The footprints of initial complexes forming with σ^{32} and σ^{70} holoenzymes demonstrate that these, like the σ^N closed complex, are shorter than the open complex footprint, not covering the initiating nucleotide position (36–39). Similarly, SP01 sigma in the presence of thymine rather than hydroxymethyluracil-containing template DNA has a short holoenzyme footprint in the absence of strand separation (40). Hence, in each of these closed complexes the core RNA polymerase subunits may not, as also appears to be the case with σ^N holoenzyme, be close to the subsequently melted DNA region until the holoenzyme has undergone a configurational change needed for open complex formation. This proposal is similar to the model of Cowing *et al.* (37).

ACKNOWLEDGEMENTS

We wish to thank Ray Dixon, Mike Merrick and Barry Smith for their comments on the paper, and Carol Sterenberg for typing.

REFERENCES

1 Gross, C.A., Lonetto, M. and Losick, R. (1992) Bacterial sigma factors. In: *Transcriptional Regulation*, eds McKnight, S.L. and Yamamoto, K.R. pp. 129–176. Cold Spring Harbor Laboratory Press, Cold Spring Harbor, NY.
2 Merrick, M.J. (1993) *Mol. Microbiol.* **10**, 903–909.
3 Lonetto, M., Gribskov, M. and Gross, C. (1992) *J. Bacteriol.* **174**, 3843–3849.
4 Kustu, S., Santero, E., Keener, J., Popham, D. and Weiss, D. (1989) *Microbiol. Rev.* **53**, 367–376.
5 Morett, E. and Buck, M. (1989) *J. Mol. Biol.* **210**, 65–77.
6 Popham, D.L., Szeto, D., Keener, J. and Kustu, S. (1989) *Science* **243**, 629–635.
7 Sasse-Dwight, S. and Gralla, J.D. (1988) *Proc. Natl. Acad. Sci. USA* **85**, 8934–8938.
8 Merrick, M. and Chambers, S. (1992) *J. Bacteriol.* **174**, 7221–7226.
9 Sasse-Dwight, S. and Gralla, J.D. (1990) *Cell* **62**, 945–954.
10 Wong, C., Tintut, Y. and Gralla, J.D. (1994) *J. Mol. Biol.* **236**, 81–90.
11 Buck, M. and Cannon, W. (1992) *Nature* **358**, 422–424.
12 Dombroski, A.J., Walter, A.W., Record, T.M., Siegele, D.A. and Gross, C.A. (1992) *Cell* **70**, 501–512.
13 Morris, L., Cannon, W., Claverie-Martin, F., Austin, S. and Buck, M. (1994) *J. Biol. Chem.* **269**, 11563–11571.
14 Tintut, Y., Wong, C., Ying, J., Hsieh, M. and Gralla, J.D. (1994) *Proc. Natl. Acad. Sci. USA* **91**, 2120–2124.
15 Cannon, W., Claverie-Martin, F., Austin, S. and Buck, M. (1993) *Mol. Microbiol.* **8**, 287–298.
16 Hsieh, M., Tintut, Y. and Gralla, J.D. (1994) *J. Biol. Chem.* **269**, 373–378.
17 Cannon, W., Claverie-Martin, F., Austin, S. and Buck, M. (1994) *Mol. Microbiol.* **11**, 227–236.
18 Dixon, W.J., Hays, J.J., Levin, J.R., Weidner, M.F., Dombroski, B.A., and Tullius, T.D. (1991) *Methods Enzymol.* **208**, 380–413.
19 Ogata, R. and Gilbert, W. (1977) *Proc. Natl. Acad. Sci. USA* **74**, 4973–4977.
20 Buck, M. and Cannon, W. (1992) *Mol. Microbiol.* 6, 1625–1630.
21 Kleiner, D., Paul, W. and Merrick, M.J. (1988) *J. Gen. Microbiol.* **134**, 1779–1784.
22 Buck, M. and Cannon, W. (1994) *Nucleic Acids Res.* **22**, 1119–1120.
23 Sasse-Dwight, S. and Gralla, J.D. (1989) *J. Biol. Chem.* **264**, 8074–8081.
24 Cannon, W. and Buck, M. (1992) *J. Mol. Biol.* **225**, 271–286.
25 Harrison, S.C. and Aggarwal, A.K. (1990) *Ann. Rev. Biochem.* **59**, 933–969.
26 Charlton, W., Cannon, W. and Buck, M. (1993) *Mol. Microbiol.* **7**, 1007–1021.
27 Minchin, S.D., Austin, S. and Dixon, R.A. (1989) *EMBO J.* **8**, 3491–3499.
28 Buck, M., Cannon, W. and Woodcock, J. (1987) *Mol. Microbiol.* **1**, 243–249.
29 Su, W., Porter, S., Kustu, S. and Echols, H. (1990) *Proc. Natl. Acad. Sci. USA* **87**, 5504–5508.
30 Hoover, T.R., Santero, E., Porter, S. and Kustu, S. (1990) *Cell* **63**, 11–22.
31 Claverie-Martin, F. and Magasanik, B. (1991) *Proc. Natl. Acad. Sci. USA* **88**, 1631–1635.
32 Lee, H.S., Ishihama, A. and Kustu, S. (1993) *J. Bacteriol.* **175**, 2479–2482.
33 Joho, K.E., Gross, L.B., McGraw, N.J., Raskin, C. and McAllister, W.T. (1990) *J. Mol. Biol.* **215**, 21–29.
34 Reskin, C.A., Diaz, G., Johno, K. and McAllister, W.T. (1993) *J. Mol. Biol.* **226**, 506–618.
35 Sousa, R., Chang, Y.J., Rose, P.J. and Wang, B.-C. (1993) *Nature* **364**, 593–599.
36 Kovacic, R.T. (1987) *J. Biol. Chem.* **262**, 13654–13661.
37 Cowing, D.W., Mecsas, J., Record, M.T.J., and Gross, C.A. (1989) *J. Mol. Biol.* **210**, 521–530.
38 Schickor, P., Metzger, W., Werel, W., Lederer, H. and Heumann, H. (1990) *EMBO. J.* **9**, 2215–2220.
39 Mecsas, J., Cowing, D.W. and Gross, C.A. (1991) *J. Mol. Biol.* **220**, 585–597.
40 Choy, H.A., Romeo, J.M. and Geiduschek, E.P. (1986) *J. Mol. Biol.* **191**, 59–73.